

supplementary materials

Table S1. Lattice parameters after structural optimization

Strain (%)	Average Pb-I bond length (Å)	Average I-Pb-I bond angle (°)	Energy (eV)
-5	3.036	170.091	-56.62
-4	3.069	170.220	-56.78
-3	3.107	170.327	-56.90
-2	3.130	170.330	-56.98
-1	3.173	170.324	-57.03
0	3.207	170.345	-57.04
1	3.239	170.329	-57.03
2	3.272	170.333	-57.00
3	3.303	170.335	-56.95
4	3.347	170.246	-56.88
5	3.395	170.122	-56.80

Table S2. Calculated bandgaps using different methods.

	Method	α -FAPbI ₃
Bandgap (eV)	PBE	1.43
	PBE+SOC	0.45
	G0W0+SOC	1.54
	Expt.	1.48 ^{1,2}

Table S3. Polarizability under different strains.

Strain (%)	Polarizability
-5	6.95
-4	6.49

-3	6.10
-2	5.78
-1	5.50
0	5.26
1	5.05
2	4.86
3	4.70
4	4.56
5	4.10

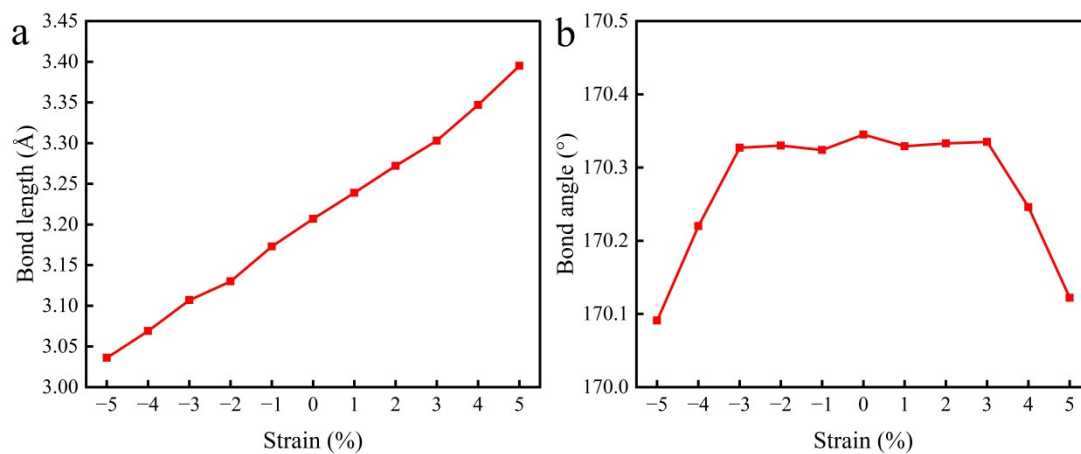


Fig. S1. (a) Average Pb-I bond length (Å) for the optimized structure

(b) Average Pb-I bond angle (°) for the optimized structure.

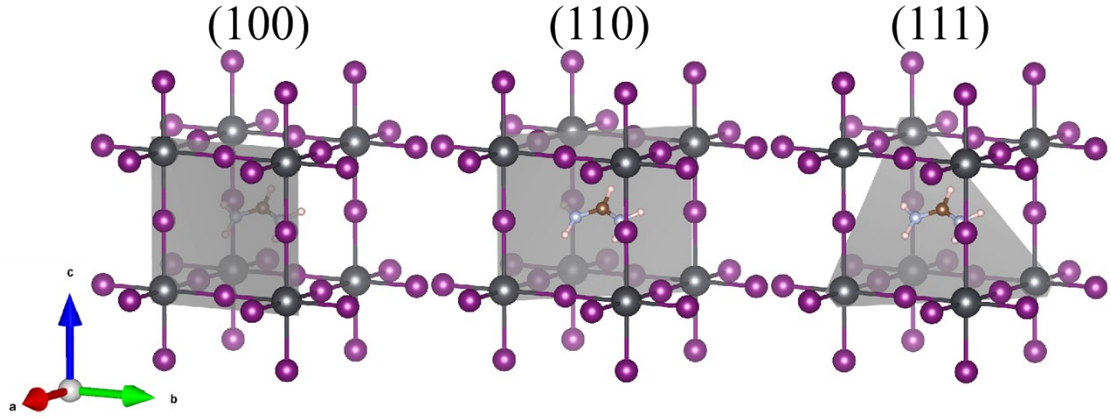


Fig. S2. Different crystal planes of α -FAPbI₃.

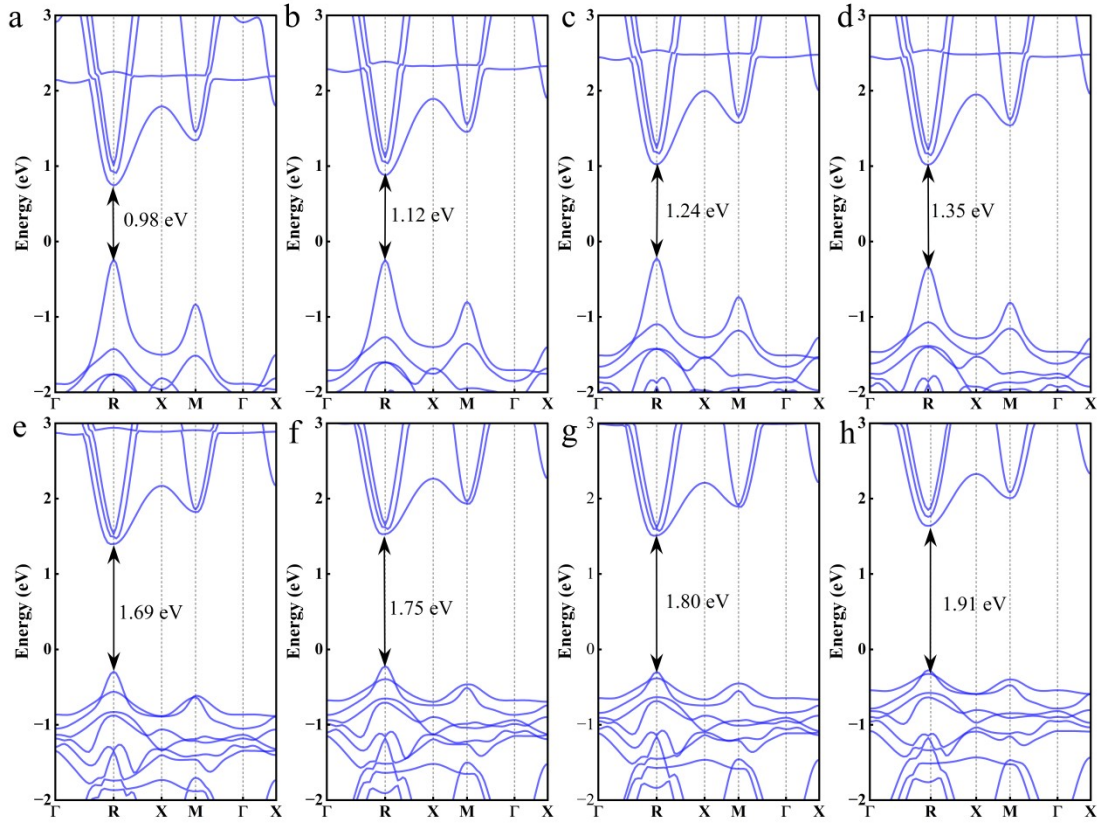


Fig. S3. The energy bands of FAPbI₃ under different strains range from -5% to -2% strain for (a-d) and from 2% to 5% strain for (e-h).

1.2 Calculation of effective mass of electrons, effective mass of holes, and exciton binding energy

To analyze carrier transport behavior, we calculated the electron effective (m_e^*), hole effective masses (m_h^*) and reduced carrier effective masses (m_r^*) by averaging

along the band-edge k -path. The effective mass is calculated using the following equations:

$$m^* = \hbar \left[\frac{d^2 E(k)}{dk^2} \right]^{-1} \quad (1)$$

$$m_r^* = \frac{m_e^* m_h^*}{m_e^* + m_h^*} \quad (2)$$

where \hbar is the reduced Planck constant, $E(k)$ is the band energy of VBM and CBM, and k is the wave vector.

The exciton binding energy arises from the Coulomb interaction between an electron and a hole, which governs the separation and recombination processes of electron-hole pairs. This energy was calculated using the formula derived from the Wannier exciton model³:

$$E_{eb} = \frac{m_r^* e^4}{2\hbar^2 \varepsilon^2} \cdot \frac{1}{(4\pi\varepsilon_0)^2} \quad (3)$$

Where m_r^* is the reduced effective mass, ε is static dielectric constant, \hbar is reduced Planck Constant, ε_0 is Vacuum permittivity.

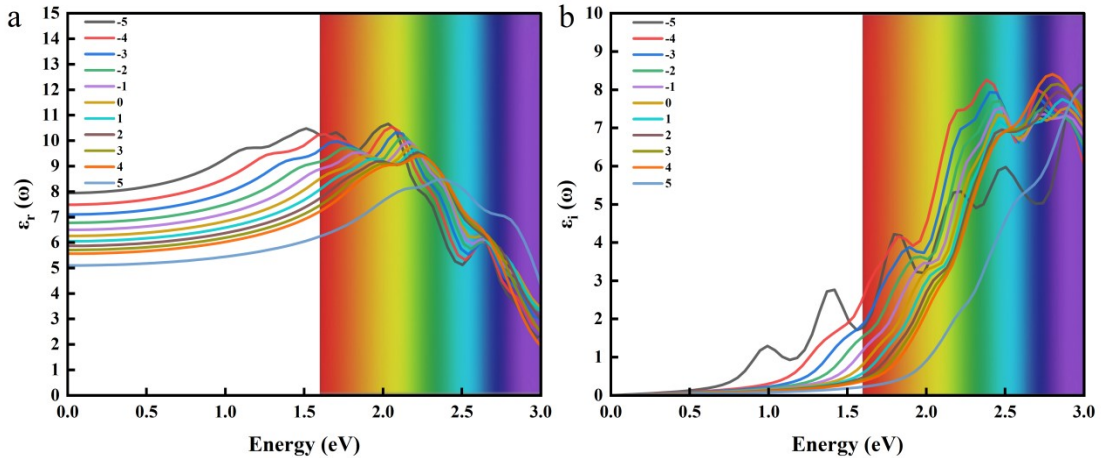


Fig. S4. (a) The real part dielectric function, (b) the imaginary part dielectric function.

1.3 Optical properties calculation

The dielectric function, a key parameter for characteristics of the optical properties of bulk materials, is defined as:

$$\varepsilon(\omega) = \varepsilon_r(\omega) + i\varepsilon_i(\omega) \quad (4)$$

Where ε_r represents the charge storage capacity and ε_i corresponds to the material's absorption and energy dissipation. To investigate the optical properties of FAPbX₃, we calculated within the 0-3 eV energy range (Fig. S3). Subsequently, we derived key optical parameters including absorption coefficient (α), refractive index (n), extinction coefficient (κ), reflectivity (R), and energy loss function (L) using the following formulas ⁴:

$$\alpha = \frac{\sqrt{2}\omega}{c} \left[\sqrt{\varepsilon_r^2 + \varepsilon_i^2} - \varepsilon_r \right]^{\frac{1}{2}} \quad (5)$$

$$n = \frac{1}{\sqrt{2}} \left[\sqrt{\varepsilon_r^2 + \varepsilon_i^2} + \varepsilon_r \right]^{\frac{1}{2}} \quad (6)$$

$$\kappa = \frac{1}{\sqrt{2}} \left[\sqrt{\varepsilon_r^2 + \varepsilon_i^2} - \varepsilon_r \right]^{\frac{1}{2}} \quad (7)$$

$$R = \frac{(n-1)^2 + \kappa^2}{(n+1)^2 + \kappa^2} \quad (8)$$

$$L = \frac{\varepsilon_i}{\varepsilon_r^2 + \varepsilon_i^2} \quad (9)$$

1.4 Calculation of transition dipole moment and joint density of states

The transition dipole moment is the matrix element of the electric dipole moment operator between quantum states, characterizing the transition strength between two energy levels. Its expression is:

$$p = \langle \psi_f | e\mathbf{r} | \psi_i \rangle \quad (10)$$

Where $|\psi_i\rangle$ is the initial state, $\langle \psi_f |$ is the final state, e is the elementary charge, \mathbf{r} is the position vector, and p^2 is proportional to the transition probability

The joint density of states (JDOS) describes the number of electron state pairs in a material that satisfy momentum and energy conservation during transitions from the valence band to the conduction band. The calculation process is as shown in the following formula.⁶

$$JDOS = \frac{1}{(2\pi)^3} \int \delta(E_c(\mathbf{k}) - E_v(\mathbf{k}) - \hbar\omega) d\mathbf{k} \quad (11)$$

Where $\delta(\cdot)$ is the Dirac delta function, enforcing energy conservation $E_c - E_v = \hbar\omega$. $E_c(\mathbf{k})$ and $E_v(\mathbf{k})$ are the energies of the conduction and valence bands at wave vector \mathbf{k} respectively, and $\hbar\omega$ is the incident photon energy. The integration spans the entire Brillouin zone.

The optical absorption coefficient α is related to JDOS and p^2 as follows:

$$\alpha \propto \frac{p^2}{\hbar\omega} \cdot JDOS \quad (12)$$

1.5 Defect properties calculation

In examining the defect formation energy (DFE) of point defects in FAPbI₃, a 2×2×2 supercell is employed, as shown in Fig. S4, with a point defect formed into the supercell to facilitate the averaging of defect volume⁷. For the calculation of charged defects, it is assumed that the additional or missing electrons from charged defects come from an external electron reservoir or enter the supercell interior, with their energy equivalent to the Fermi energy, using the equation⁸:

$$DFE = E(\text{defect}) - E(\text{perfect}) + \sum_i n_i \mu_i + q(E_F + E_{VBM}) + E_{corr} \quad (13)$$

$$E_{corr} = \frac{q^2 \alpha_M}{2\epsilon L} + \frac{2\pi q Q}{3\epsilon L^3} \quad (14)$$

Where $E(\text{defect})$ represents the system containing defects, $E(\text{perfect})$ is the energy of the perfect system without defects; n and μ are the number of atoms and the corresponding chemical potentials, individually. For vacancy defects, $n_i > 0$, and for interstitial defects, $n_i < 0$. In order to ensure the formation of perovskite, the chemical potentials of FA, Pb, and I satisfy the following relationship:

$$\mu_{FA} + \mu_{Pb} + 3\mu_I = \Delta H(\text{FAPbI}_3) \quad (15)$$

Here, ΔH represents the formation energy of perovskite in the cubic phase. We selected the cubic phase of Pb solid, the orthorhombic phase of I_2 solid, and the cubic phase of FA to calculate their chemical potentials respectively. In order to prevent the formation of FAI and PbI_2 as by-products, it is necessary to ensure that the chemical potential values satisfy the following conditions:

$$\mu_{FA} + \mu_I < \Delta H(\text{FAI}) \quad (16)$$

$$\mu_{Pb} + 2\mu_I < \Delta H(\text{PbI}_2) \quad (17)$$

In accordance with equations (2) - (4), the chemical potential regions under equilibrium growth conditions for the perovskite were calculated. In this research, the moderate chemical potentials of FA, Pb, and I were selected for calculating DFE. The last term $q(E_F + E_{VBM}) + E_{corr}$, q represents the charge of the defect; E_{VBM} represents the energy level at the top of the valence band; E_F is the Fermi-level at the top of its relative valence band, the top of the valence band $E_F = 0$, the Fermi-level are permitted to fluctuate within the band gap, with the upper limit of the valence band maximum (VBM) aligned with the lower limit of the conduction band minimum (CBM) in a defect-free $FAPbI_3$ crystal, which serves as the reference point for the band gap; E_{corr} is a correction term added to avoid spurious interactions of charged defects between supercells so that the potential energy in the defective supercells corresponds to the bulk potential energy.^{9, 10} The specific correction scheme employed in this work was the Makov–Payne (MP) correction,¹¹ expressed as equation 14, where α_M denotes the Madelung constant for the finite supercell geometry, ε represents the static dielectric constant of the material, and L corresponds to the characteristic dimension of the supercell.

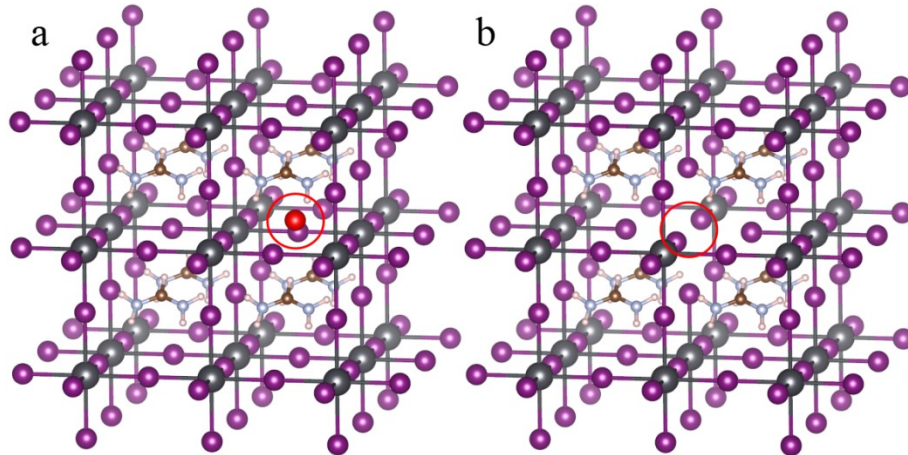


Fig. S5. (a) Interstitial defects and (b) vacancy defects in a $2 \times 2 \times 2$ FAPbI₃ super cell.

1.6 Diffusion coefficient and ionic mobility

Molecular dynamics simulations were conducted using the NVT ensemble (canonical ensemble) with a Langevin thermostat at 300K,^{12, 13} employing a time step of 1 fs for a total duration of 10 ps. Accurate root-mean-square displacement (RMSD) calculations required a 5 ps equilibration period before analysis.

The mean square displacement (MSD) is defined as the average of the square of the displacement of a particle over a given time interval. Its direct relationship with the diffusion coefficient D is governed by the Einstein relation¹⁴:

$$D = \frac{1}{6} \lim_{\Delta t \rightarrow \infty} \frac{d(\text{MSD})}{d\Delta t} \quad (18)$$

When the MSD exhibits linear growth with time (in the diffusive regime), the slope corresponds to $6D$, i.e., $\text{MSD} = 6D\Delta t$.

The relationship between the diffusion coefficient and ionic mobility is established by the Nernst-Einstein relation¹⁵:

$$\mu = \frac{Dq}{k_B T} \quad (19)$$

References

1. A. Pisanu, C. Ferrara, P. Quadrelli, G. Guizzetti, M. Patrini, C. Milanese, C. Tealdi and L. Malavasi, *The Journal of Physical Chemistry C*, 2017, **121**, 8746-8751.
2. J. H. Noh, S. H. Im, J. H. Heo, T. N. Mandal and S. I. Seok, *Nano Lett.*, 2013, **13**, 1764-1769.
3. J. Even, L. Pedesseau and C. Katan, *The Journal of Physical Chemistry C*, 2014, **118**, 11566-11572.
4. Q. Qi, H. Fu, Y. Li, H. Cai, X. Wu and C. Zhong, *J. Power Sources*, 2025, **630**, 236135.
5. Y. Tang, Q. Xie, X. Zhang, J. Ma, H. Xie, Y. Liu, L. Zhao, D. Yan, X. Wang and W. Ye, *Laser Photonics Rev.*, 2025, DOI: 10.1002/lpor.202500430.
6. C. I. Cabrera, D. A. Contreras-Solorio and L. Hernández, *Physica E*, 2016, **76**, 103-108.
7. Y. N. Wu, X. G. Zhang and S. T. Pantelides, *Phys. Rev. Lett.*, 2017, **119**, 105501.
8. W.-J. Yin, T. Shi and Y. Yan, *Appl. Phys. Lett.*, 2014, **104**, 063903.
9. C. Freysoldt, J. Neugebauer and C. G. Van de Walle, *Phys. Rev. Lett.*, 2009, **102**, 016402.
10. H. P. Komsa and A. Pasquarello, *Phys. Rev. Lett.*, 2013, **110**, 095505.
11. G. Makov and M. C. Payne, *Physical Review B*, 1995, **51**, 4014-4022.
12. W. G. Hoover, A. J. C. Ladd and B. Moran, *Phys. Rev. Lett.*, 1982, **48**, 1818-1820.
13. D. J. Evans, *The Journal of Chemical Physics*, 1983, **78**, 3297-3302.
14. E. W. Woolard, A. Einstein, R. Furth and A. D. Cowper, *The American Mathematical Monthly*, 1928, **35**, 2298685.
15. Z. Li, R. P. Misra, Y. Li, Y.-C. Yao, S. Zhao, Y. Zhang, Y. Chen, D. Blankschtein and A. Noy, *Nat. Nanotechnol.*, 2022, **18**, 177-183.